Design and Modeling of Mid-Infrared Transistor-Injected Quantum Cascade Lasers

Kanuo Chen and John Dallesasse

Department of Electrical and Computer Engineering, University of Illinois at Urbana-Champaign, Urbana, IL, 61801
Tel: +1(217)333-8416. Email:jdallesa@illinois.edu

Keywords: Quantum Cascade Laser, Transistor Laser, Gallium Arsenide, Aluminum Gallium Arsenide

Abstract

A novel coherent mid-infrared emission source, the transistor-injected quantum cascade laser, is designed and modeled. Band engineering of the quantum cascade laser ensures desired lasing wavelength and a plasmon-enhanced waveguide is employed to confine the optical field. By incorporating the quantum cascade lasing region into a conventional heterojunction bipolar transistor, independent control of current and field through the lasing region is achieved. Higher differential quantum efficiency and lower threshold current density are also predicted.

INTRODUCTION

Recently, the demand for chemically selective detection of molecular trace gases has been increasing dramatically in many application areas, such as environmental gas monitoring, industrial process control and medical diagnostics. Since the absorption of many target gas molecules peak in the mid-infrared range, infrared laser spectroscopy has become a well-suited technique for trace gas monitoring and has yielded many important results using tunable laser-based sources. Among all the mid-infrared light sources for chemical sensing, quantum cascade lasers (QCL) offer unique advantages including high output power, narrow spectral linewidth, compactness and low cost [1,2]. One prospective real world application is in situ plasma process monitoring and control. Thanks to the fine spectral range of the quantum cascade laser, the absorption spectrum of molecule species can be measured precisely [3]. By employing a feedback control loop, the gas flow in a process chamber can be made more stable. This technique has been applied to in situ process monitoring during the industrial production of DRAMs [4].

Conceptually different from a traditional semiconductor diode laser, quantum cascade lasers are unipolar semiconductor lasers with stimulated emission based upon electron inter-subband transitions [5-8]. Without the limitation of the energy bandgap, band engineering enables great flexibility of the lasing wavelength. Hence, the quantum cascade laser has become an important coherent light source in the mid-infrared regime. However, as a two-terminal device, the coupled control of current and field within the lasing active region suppresses the performance of the laser. At certain current injection levels the voltage drop across the device alters the upper and lower lasing levels and light output at designed wavelength is no longer guaranteed.

Another novel photonic device is the transistor laser, invented in 2004 [9-12]. By inserting quantum wells into the base region of a bipolar transistor and utilizing electron-hole recombination, stimulated emission can be realized in a three-terminal device.

The idea of the transistor laser inspired the use of a three-terminal structure, the transistor-injected quantum cascade laser (TI-QCL), to address the inherent issues with the quantum cascade laser [13-15]. By incorporating a quantum cascade lasing core in the base-collector junction of an n-p-n bipolar transistor, separate control of the current through the lasing active region and the applied bias across it can be achieved. The injection current of the lasing core comes from the emitter while the base-collector voltage provides the bias across the quantum cascade region. The decoupled current-voltage control enables more stable light output as the electron bound states in the conduction band are free of the field-induced modification that occurs in a conventional two-terminal QCL structure when changing the bias.

Moreover, the TI-QCL also has lower free carrier absorption compared with a conventional QCL. Traditional quantum cascade lasers have an n+-i-n configuration. The intrinsic lasing active region lies between two heavily doped n-type semiconductors; hence the laser suffers from large free carrier absorption. In the TI-QCL the intrinsic lasing region is incorporated into a lightly doped p-type base and an n-type collector. This lower doping level enables a much lower free carrier absorption in the transistor-injected quantum cascade laser. Threshold current density decreases and differential quantum efficiency increases accordingly.

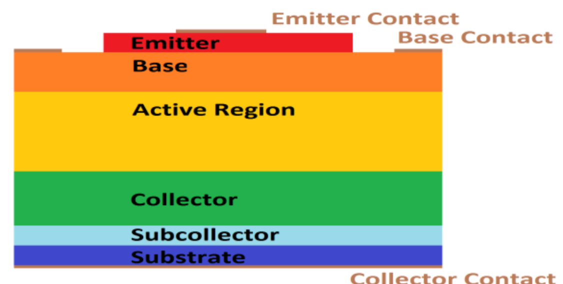

Figure 1. Cross sectional illustration of the TI-QCL

Based upon this concept, the transistor-injected quantum cascade laser is designed and modeled. Band engineering is optimized with a Schrödinger-Poisson Rate Equation solver. The optical waveguide structure is designed, simulated and improved. The electrical merit of the transistor is also simulated.

OVERALL DESIGN

As is mentioned above, the design of the transistor-injected quantum cascade laser involves inserting the conventional quantum cascade laser into the base-collector junction of the heterojunction bipolar transistor. A device cross-sectional illustration can be found in Fig. 1. The structure contains an InGaP emitter which is heavily n-type doped, a lightly C-doped GaAs base, and an intrinsic GaAs/AlGaAs quantum cascade lasing region followed by a Si-doped GaAs collector on a GaAs substrate.

The band diagram illustration of the TI-QCL can be found in Fig. 2. Turning on the transistor-injected quantum cascade laser requires forward bias of the emitter-base junction and reverse bias of the base-collector junction. Under forward bias electrons are injected from the emitter and then transit through the base into the base-collector junction while emitting photons within the intrinsic quantum cascade regions. Finally, electrons are collected at the collector and conducted away.

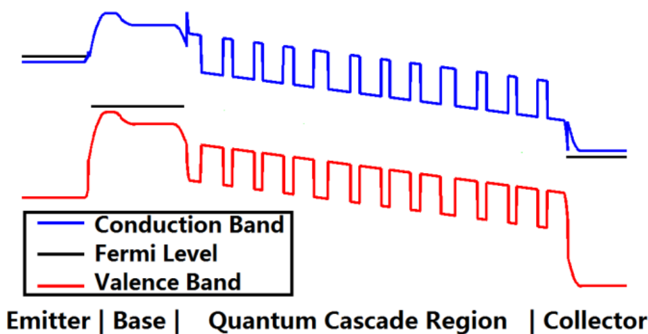

Figure 2. Band diagram illustration of the TI-QCL.

BAND ENGINEERING OF THE QUANTUM CASCADE LASING REGION

Compared with traditional semiconductor diode lasers which depend on electron-hole recombination across the bandgap, quantum cascade lasers rely on electron transitions between subbands within the conduction band. Hence, band engineering is crucial to a quantum cascade laser since it fully determines the lasing wavelength. In order to optimize the design of the lasing active region, a self-consistent Schrödinger-Poisson Rate Equation solver (SPRE solver) is developed. For a proposed lasing active region design, the SPRE solver first uses the Transfer Matrix method to solve the Schrödinger equation:

$$\left[-\frac{\hbar^2}{2}\frac{d}{dz}\left(\frac{1}{m^*(z)}\frac{d}{dz}\right)+V(z)\right]\psi(z)=E\psi(z) \qquad (1)$$

Here, $m^*(z)$ is the position-dependent effective mass of electron and $V(z)$ is the potential seen by electrons. The potential $V(z)$ contains two parts, one is the piecewise conduction band edge resulting from the alternating quantum wells and barriers; the other is introduced due to doping and the occupation of electrons in subbands. While the former is numerically easy to obtain, the latter can be found by solving the Poisson equation:

$$-\frac{d}{dz}\left[\varepsilon(z)\frac{d}{dz}\varphi(z)\right]=e\left[N(z)-\sum_n n_n\,|\psi_n(z)|^2\right] \qquad (2)$$

Here $-e\varphi$ represents the electric potential attributed to the doping concentration $N(z)$ and the accumulation of electrons in the subbands. The electron wavefunction of the n-th subband ψ_n is obtained by the Schrödinger equation. The concentration of electrons in the n-th subband under injection denoted as n_n can be found by solving the rate equation using the Runge-Kutta method. By solving the Schrödinger-Poisson rate equation iteratively, a self-consistent solution of electron wavefunctions, eigenenergies and electron population on each bound state is obtained.

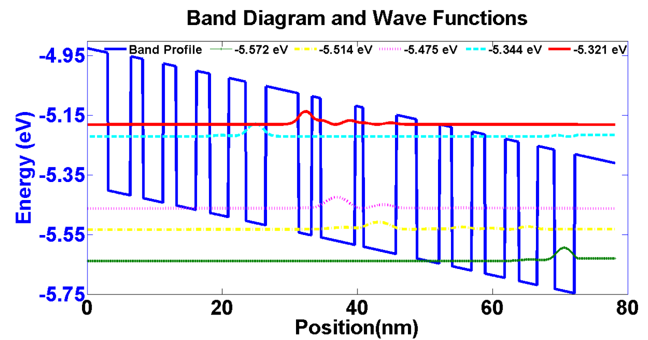

Figure 3. Optimized lasing active region design of the TI-QCL and electron wavefunctions within the conduction band.

Fig. 3 shows the band engineering optimization result of a GaAs/AlGaAs active region design under a 4.8kV/cm electric field and the electron wavefunctions within the conduction band. In the lasing core of a quantum cascade laser there are many identical stages of alternating quantum wells and barriers which form repetitive sets of injector and active region. In Fig. 3 the band diagram starts with an injector, then the lasing active region consisting of three quantum wells and then is followed by the injector of the next identical stage. The layer sequence in nanometers from the left is **2.8**/3.4/**1.7**/3.0/**1.8**/2.8/**2.0**/3.0/**2.6**/3.0/**4.6**/1.9/**1.1**/ 5.4/**1.1**/4.8/**2.8**/3.4/**1.7**/3.0/**1.8**/2.8/**2.0**/3.0/**2.6**/3.0/**4.6.** The barrier is made of AlGaAs with 65% Al shown in bold while the quantum well is made of GaAs. From the top to the bottom are the upper lasing level, the left injector state, the lower lasing level, the depopulation level and the right

injector level. Electrons are injected into the left injector state and tunnel through the injection barrier via resonant tunneling into the upper lasing level. The lasing transition occurs and the lasing wavelength is 8.05μm. Electrons on the lower lasing level are then depopulated through strong electron-phonon interaction into the depopulation level and enter the next stage of lasing active region from the right injector level.

Using Fermi's Golden rule, the electron-electron interaction is calculated in the lasing active region [16]. The electron-phonon interaction is described by the superlattice Frohlich model [17]. These scattering events tend to redistribute electrons in each subband, and at steady state electron population on each level reach a quasi-equilibrium. This process is simulated by solving the rate equation. Within one stage of the injector and active region, the population evolution of the four key states as a function of time are shown in Fig. 4. Here the relative tolerance is 1e-3 and the simulation temperature is 300K. As the lasing core of the transistor-injected quantum cascade laser is repeated, the electron concentration of one stage is sufficient to represent the full structure.

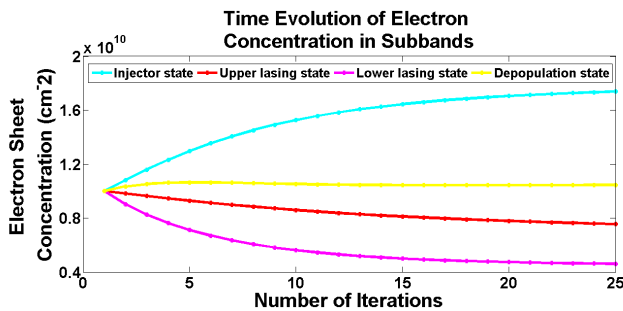

Figure 4. Simulation of the rate equation. The time step is 0.05ps and relative tolerance is 1e-3. The simulation converges after 25 iterations.

From the steady state electron population it is found that the transistor-injected quantum cascade laser suffers from one third less free carrier absorption compared with a conventional quantum cascade laser containing the same active region design. The threshold current density is also reduced by approximately 20%.

CLADDING-COMBINED PLASMON-ENHANCED OPTICAL WAVEGUIDE DESIGN

Since the material chosen for the lasing active region is GaAs/AlGaAs, the design of an optical waveguide based upon a GaAs substrate is crucial to laser performance. Here a cladding-combined plasmon-enhanced waveguide is proposed to suppress the leakage of the optical field into the doped region. Plasmon-enhanced waveguides are a popular choice in designing waveguide structures for conventional quantum cascade lasers [18]. The heavy doping concentration in an n-type semiconductor in the QCL leads to a large reduction of the real part of the refractive index due to plasmon resonance. By inserting cladding layers between the intrinsic lasing active region and heavily n-type semiconductor, the plasmon-enhanced waveguide provides the mid-infrared quantum cascade lasers an optical confinement factor of generally no more than 50%.

In the design of the optical waveguide in the TI-QCL however, a different but more effective waveguide design matched the transistor structure of the laser is proposed. Below the emitter cap a top cladding layer of AlGaAs with 90% Al concentration is used. What's below the top cladding is the essence of the TI-QCL, the emitter, the base, the quantum cascade lasing core and the collector. Between the subcollector and the substrate there is a bottom cladding layer which has the same composition as the top. The InGaP emitter has an n-type doping level of 2e17 $cm^{-3,}$ which strongly decreases the real part of the refractive index to 2.3. The top and bottom cladding layer further confines the optical field resulting in an optical confinement factor of 68%. The refractive index profile of the transistor-injected quantum cascade laser can be found in Fig. 5. The optical field distribution is simulated with COMSOL Multiphysics and the normalized electric field magnitude in cross section can be found in Fig. 6.

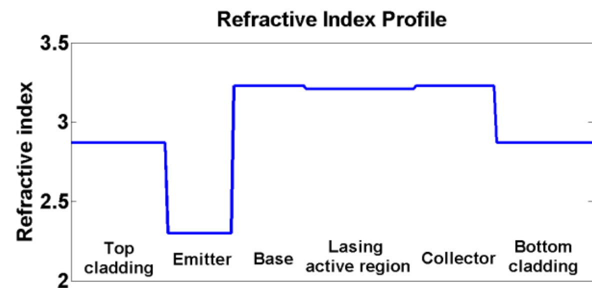

Figure 5. Refractive index profile of the TI-QCL in direction perpendicular to the layers

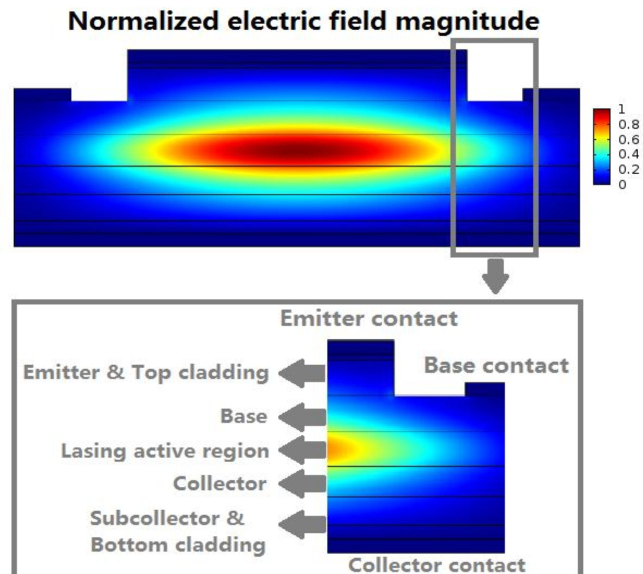

Figure 6. Normalized electric field magnitude in the cross section of the TI-QCL. From the top: contact, top cladding, emitter, base, quantum cascade lasing active region, collector, subcollector, bottom contact and substrate.

ELECTRICAL MODELING OF THE TRANSISTOR

How the TI-QCL behaves from the aspect of a heterojunction bipolar transistor is important since it determines the current-voltage relation of the laser. The electrical properties of the transistor are examined using Synopsys TCAD. By assigning equivalent material parameters for the lasing active region, the collector current and collector-emitter voltage relation is simulated for a given base current. The transistor family of curves of a 23μm by 1mm TI-QCL can be found in Fig. 7.

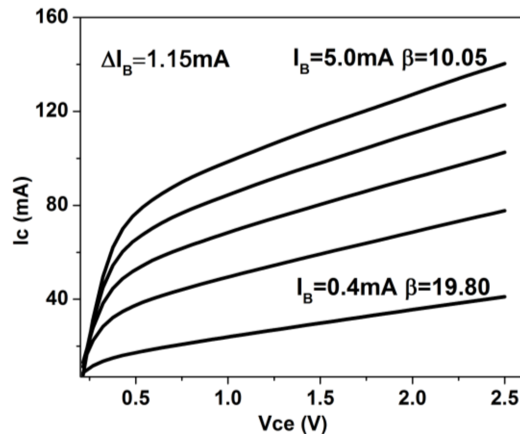

Figure 7. The transistor family of curves of the TI-QCL.

CONCLUSIONS

A new type of mid-infrared semiconductor laser, the transistor-injected quantum cascade laser, is proposed, designed and modeled. Optimization has been done regarding the design of the lasing active region to achieve the desired lasing wavelength. By using the cladding combined plasmon-enhanced waveguide the optical field is well confined and the free carrier absorption is reduced. The device electrical characteristic is also modeled. Overall, the transistor-injected quantum cascade laser is predicted to have one third lower free carrier absorption and 20% less threshold current density compared with a conventional quantum cascade laser having the same active region design.

ACKNOWLEDGEMENTS

The author would like to thank her advisor, Prof. John Dallesasse, and her co-workers for their guidance and help.

REFERENCE

[1] A. Kosterev, F. Tittel, *IEEE J. Quantum Electron*. **38**(6), 582 (2002)

[2] A. Kosterev, G. Wysocki, Y. Bakhirkin, S. So, R. Lewicki, M. Fraser, F. Tittel, R. Curl, *Appl. Phys. B*. **90**, 165 (2008)

[3] N. Lang, J. Ropcke, S. Wege, A. Steinbach, *EPJ Appl. Phys*. **49**, 13110 (2010)

[4] N. Lang, J. Ropcke, A. Steinbach, S. Wege, *IEEE Trans. Plasma Sci*. **37** (Part 2) (2009)

[5] J. Faist, F. Capasso, D. L. Sivco, C. Sirtori, A. L. Hutchinson, and A. Y. Cho, Science **264**, 553 (1994).

[6] J. Faist, F. Capasso, C. Sirtori, D. L. Sivco, J. N. Baillargeon, A. L. Hutchinson, and A. Y. Cho, *Appl. Phys. Lett.* **68**, 3680 (1996).

[7] G. Scamarcio, F. Capasso, C. Sirtori, J. Faist, A. Hutchinson, D. Sivco and A. Cho, *Science* **276**, 773 (1997).

[8] J. Faist, M. Beck, T. Aellen, and E. Gini, *Appl. Phys. Lett.* **78**, 147 (2001).

[9] G. Walter, N. Holonyak, Jr., M. Feng, and R. Chan, *Appl. Phys. Lett.* **85**, 4768 (2004).

[10] M. Feng, N. Holonyak, Jr., G. Walter, and R. Chan, *Appl. Phys. Lett.* **87**, 131103 (2005).

[11] M. Feng, N. Holonyak, Jr., R. Chan, A. James, and G. Walter, *Appl. Phys. Lett.* **88**, 063509 (2006).

[12] M. Feng, N. Holonyak, Jr., H. W. Then, C. H. Wu, and G. Walter, *Appl. Phys. Lett.* **94**, 041118 (2009).

[13] K. Chen, J. M. Dallesasse, "The Transistor-Injected Quantum Cascade Laser: A Novel Mid-IR Emitter" *55th Electronic Material Conference*, (2013)

[14] K. Chen, J. M.Dallesasse, "Theory and Modeling of the Transistor-Injected Quantum Transition Laser: A Mid-IR and THz Coherent Source" *11th Annual CNST Nanotechnology Workshop*, (2013)

[15] J. M. Dallesasse, *2013 European Microwave Conference Workshop* W12: Terahertz Technologies, (2013).

[16] P. Harrison, *Quantum Wells, Wires and Dots: Theoretical and Computational Physics of Semiconductor Nanostructures,* 2nd ed. New York: Wiley (2005).

[17] K. Huang and B. Zhu, *Phys. Rev. B* **38**, 13 377 (1988).

[18] C. Sirtori, P. Kruck, S. Barbieri, P. Collot, J. Nagle, M. Beck, J. Faist and U. Oesterle, *Appl. Phys. Lett*. **73**, 3486 (1998)

ACRONYMS

QCL: Quantum Cascade Laser
TL: Transistor Laser
HBT: Heterojunction Bipolar Transistor
TI-QCL: Transistor-Injected Quantum Cascade Laser
InGaP: Indium Gallium Phosphide
GaAs: Gallium Arsenide
AlGaAs: Aluminum Gallium Arsenic